PROCEEDINGS OF SCIENCE

Extracting properties of the T_{cc} state from lattice QCD

Vadim Baru[a,*]

[a] *Institut für Theoretische Physik II, Ruhr-Universität Bochum, D-44780 Bochum, Germany*

E-mail: vadimb@tp2.rub.de

A brief overview of the properties of the exotic state T_{cc}, as extracted from the LHCb data and lattice QCD simulations using chiral effective field theory (χEFT), is presented. We demonstrate that explicit account for the longest-range one-pion exchange interaction, including the energy scales associated with the three-body and left-hand cuts, is crucial to maintaining the correct analytic structure of the DD^* scattering amplitude near the threshold. Using χEFT up to next-to-leading order, we extract the low-energy DD^* scattering amplitude from data at both physical and unphysical pion masses and predict the light-quark mass dependence of the T_{cc} pole position. All properties of the T_{cc} state inferred from the data strongly support its molecular nature.

QNP2024 – *10th International Conference on Quarks and Nuclear Physics*
8–12 July 2024
Universitat de Barcelona, Barcelona, Spain

*Speaker

PoS(QNP2024)043

1. Introduction

In recent years, significant progress has been made in the spectroscopy of exotic hadrons containing heavy quarks, especially with the discovery of numerous exotic multiquark states, as summarized in recent reviews [1–8]. These states, which do not fit into the traditional quark model, include mesonic tetraquarks and baryonic pentaquarks, many of which are found near hadron-hadron thresholds. Among these, the discovery of the doubly-charmed exotic resonance $T_{cc}(3875)^+$ by the LHCb experiment [9, 10] has attracted considerable attention. This state, with a minimal quark content of $cc\bar{u}\bar{d}$, is located just below the $D^{*+}D^0$ threshold, and its narrow width is predominantly determined by the strong decay to $DD\pi$.

The theoretical understanding of such exotic states is still evolving, with various models proposing different internal structures. One promising scenario suggests that some of these states, like the T_{cc}, may be hadronic molecules, formed by the interaction of two hadrons such as D and D^*. The size of these hadronic molecules is controlled by the binding energy, with the T_{cc} expected to be a large-size state, unlike compact multiquark configurations. Various approaches, including effective field theory (EFT) [11–16] and phenomenological analyses (see, e.g., [7] and references therein), have been employed to understand the properties of the T_{cc}, with studies focusing on its pole extraction and decay characteristics.

Significant progress in the study of exotic states has recently been achieved in lattice QCD [17–21], see in particular Refs. [22–27] in the context of DD^* scattering. However, it has also become clear that extracting infinite-volume observables from lattice energy levels, especially the pole positions for near-threshold states, is challenging due to the presence of nearby left-hand cuts (lhcs) arising from long-range interactions like one-pion exchange (OPE) [28–31]. Consequently, several extensions of the Lüscher method or alternative approaches have been proposed to address this issue [28, 31–33]. Additionally, the effective range expansion (ERE), commonly used to parameterize the near-threshold energy behavior of the inverse scattering amplitude, is only suitable in the absence of nearby lhcs [34].

In this Proceeding, we summarize these challenges and show how they can be overcome using a chiral EFT-based approach (χEFT) that incorporates the effects of the OPE. Applying this method to lattice QCD data, we resolve the lhc issues that the standard Lüscher method faces in cases with significant long-range interactions. This allows us to extract infinite-volume observables from lattice energy levels, even in the presence of lhcs [31]. Using the T_{cc} pole positions, that we extracted from the experiment [13] and lattice data at a pion mass of $m_\pi = 280$ MeV [31], we then predict the T_{cc} pole trajectory in chiral EFT as a function of the light-quark mass [35], see also [37, 38] for related works on the $X(3872)$ within the same framework.

2. Chiral EFT approach for two heavy mesons

The scattering T-matrix in the physical world and also in the infinite-volume for the larger than physical pion masses can be obtained by solving the LSE in the partial wave basis, see Fig. 1 for the graphical illustration, as follows:

$$T_{\alpha\beta}(E,p,p') = V_{\alpha\beta}(p,p') + \int \frac{d^3q}{(2\pi)^3} V_{\alpha\gamma}(k,q) G(E,q) T_{\gamma\beta}(E,q,p'),$$

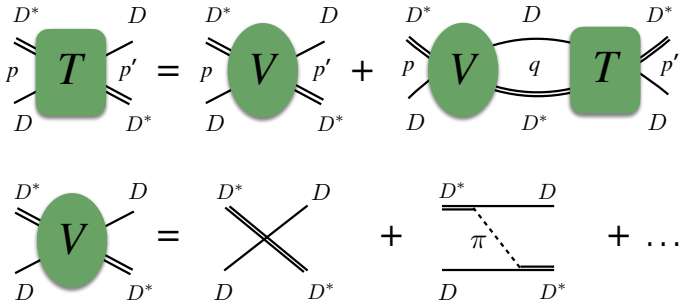

Figure 1: Graphical illustration of the Lippmann-Schwinger equations solved in the infinite-volume. The effective potential consists of the $O(Q^2)$ contact interactions from Eq. (1) and the one-pion exchange Eq.(2).

where α and β refer to the partial waves, and E is the total energy. Here, $G(E,q)$ is the DD^* Green function, including the self energy of the D^*, see Refs. [13, 35] for the explicit expression.

The effective potential V for DD^* scattering is incorporated within chiral EFT up to order $O(Q^2)$, where $Q = p/\Lambda_b$. Here, p represents a characteristic low-momentum scale, either $\sim m_\pi$ or a coupled-channel momentum, while Λ_b is the chiral expansion's breakdown scale. This potential is expressed as

$$V = V^{(0)}_{\rm OPE} + V^{(0)}_{\rm cont} + V^{(2)}_{\rm cont} + \ldots,$$

with contributions from one-pion exchange (OPE) and contact terms. Two-pion exchange effects are assumed to be captured largely by the contact terms, as suggested by explicit calculations [36], where it is demonstrated that nonanalytic terms are suppressed.

The contact terms, incorporated to account for short-range dynamics, are polynomial in the pion mass and momenta. For the $J^P = 1^+$ $S-$wave contact potential ($^3S_1$ partial wave) we use

$$V_{\rm cont}(p,p') = V^{(0)}_{\rm cont} + V^{(2)}_{\rm cont} = \left[c_0(\xi) + c_2(\xi)(p^2+p'^2)\right](\boldsymbol{\epsilon}\cdot\boldsymbol{\epsilon}'^*), \tag{1}$$

where $c_0(\xi) = C_0 + D_2(\xi^2-1) + O(\xi^4, p^4)$ and $c_2(\xi) = C_2 + O(\xi^2)$, with the low-energy constants C_0, C_2 and D_2 being adjusted to data. Further, $\xi = m_\pi/m^{\rm ph}_\pi$, and $\boldsymbol{p}$ ($\boldsymbol{p}'$) and $\boldsymbol{\epsilon}$ ($\boldsymbol{\epsilon}'$) are the initial (final) D^* meson momentum and polarization, respectively.

In time-ordered perturbation theory (TOPT), the DD^* isoscalar OPE potential is ($\boldsymbol{q} = \boldsymbol{p} + \boldsymbol{p}'$)

$$V_{\rm OPE}(E,\boldsymbol{p},\boldsymbol{p}') = -\frac{g^2}{24 f_\pi^2}(\boldsymbol{\tau}^{(1)}\cdot\boldsymbol{\tau}^{(2)})\frac{(\boldsymbol{q}\cdot\boldsymbol{\epsilon})(\boldsymbol{q}\cdot\boldsymbol{\epsilon}'^*)}{2\omega_\pi(\boldsymbol{q}^2)}\Big(D_1(E,\boldsymbol{p},\boldsymbol{p}') + D_2(E,\boldsymbol{p},\boldsymbol{p}')\Big), \tag{2}$$

where f_π is the pion decay constant, g is the pion coupling constant, and the TOPT propagators D_1 and D_2 read

$$D_1(E,\boldsymbol{p},\boldsymbol{p}') = \left(2M_D + \frac{p^2+p'^2}{2M_D} + \omega_\pi(\boldsymbol{q}^2) - E - i\epsilon\right)^{-1}, \tag{3}$$

$$D_2(E,\boldsymbol{p},\boldsymbol{p}') = \left(2M_{D^*} + \frac{p^2+p'^2}{2M_{D^*}} + \omega_\pi(\boldsymbol{q}^2) - E - i\epsilon\right)^{-1}. \tag{4}$$

Further, $(\boldsymbol{\tau}^{(1)}\cdot\boldsymbol{\tau}^{(2)}) = 3$ and 1 for isoscalar and isosvector DD^* scattering, respectively. The pion is treated relativistically with $\omega_\pi(\boldsymbol{q}^2) = \sqrt{m_\pi^2 + \boldsymbol{q}^2}$, while $D^{(*)}$ mesons are treated nonrelativistically.

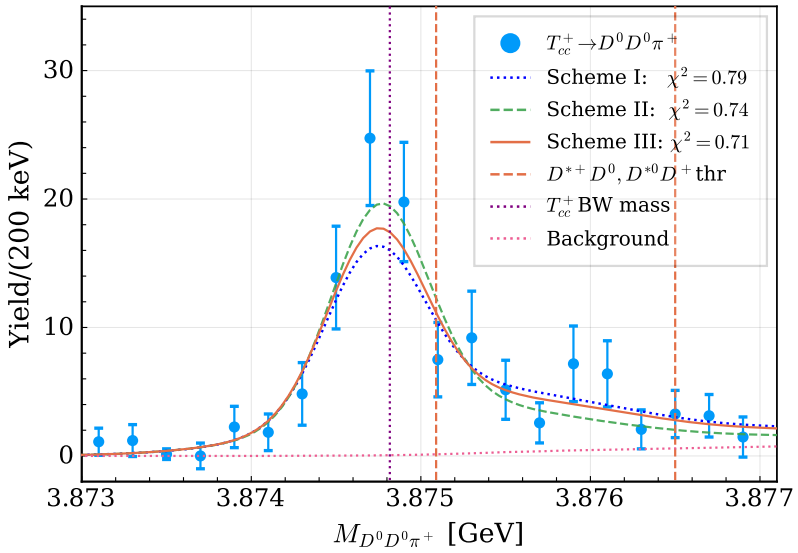

Figure 2: Fitted line shapes including the energy resolution function–see Ref. [13] for details. In constrast to Schemes I and II, the results of Scheme III incorporate the three-body cut completely.

The partial-wave projections $V_{\alpha\beta}(E, p, p')$ follow the method of Refs. [39, 40] as detailed in Ref. [35]. We note that both the OPE potential and the Green function $G(E, q)$ include the three-body cut. The branch point of this cut, found by setting $p = p' = 0$ in Eq. (3), is located at $k^2_{\text{rhc}_3} = 2\mu(m_\pi - \Delta M)$, where μ is the reduced mass of the DD^* system, and $\Delta M = M_{D^*} - M_D$. For the pion masses $m_\pi < \Delta M$, which include the range of m_π up to a few percent larger than m_π^{ph}, the three-body cut appears below the two-body threshold, allowing for the T_{cc} to decay.

3. T_{cc} properties from experimental data

In Ref. [13], the approach formulated above[1] was applied to analyze LHCb data [9, 10]. However, these data do not allow for independent determination of the momentum-dependent $O(Q^2)$ LEC C_2 due to a strong correlation with C_0. Consequently, an excellent description of the experimental line shapes was achieved by setting $C_2 = 0$, as shown in Fig. 2. To obtain this line shape, a pointlike production was assumed, as detailed in Ref. [13], with C_0 and overall normalization as the only fit parameters. The main result of the analysis was the extraction of the T_{cc} pole, yielding $-356^{+39}_{-38} - i(28 \pm 1)$ keV. While the pole's real part showed only mild sensitivity to three-body effects, given the experimental precision, its imaginary part was, as expected, dominated by the three-body $DD\pi$ cut. Additionally, effective range parameters and the compositeness [41] were evaluated, strongly supporting the molecular nature of this state, see also Ref. [42] for additional discussions.

4. Analysis of lattice data at $m_\pi = 280$ MeV in chiral EFT

In Ref. [31], a chiral EFT-based approach was proposed, for the first time, to extract information on two-body scattering from finite-volume (FV) energy levels. Compared to the Lüscher method, its

[1] Due to the narrow energy range used in the analysis, pions were treated nonrelativistically here.

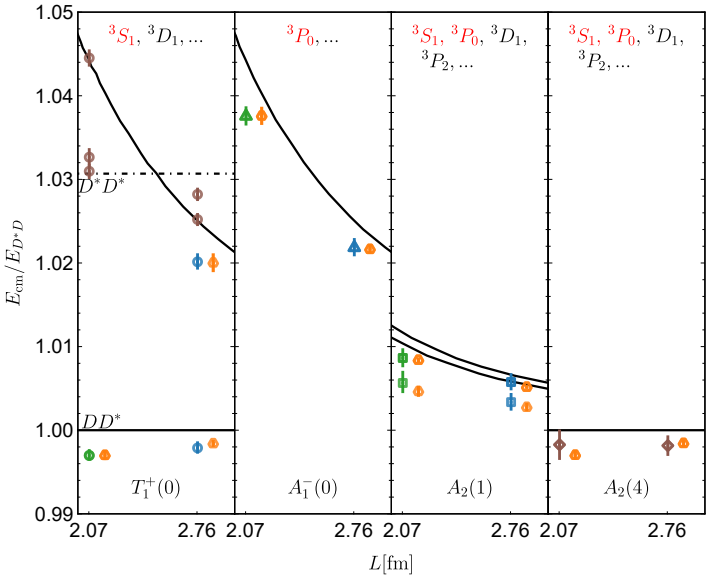

Figure 3: Fit results for the center-of-mass energy $E_{\rm cm}$ of the DD^* system normalized by $E_{DD^*} = M_D + M_{D^*}$ in various finite volume irreps. The lattice energy levels from Ref. [22] are shown by open circles, squares and triangles: the blue and green points in the irreps $T_1^+(0)$, $A_1^-(0)$ and $A_2(1)$ are used as input. The orange symbols, slightly shifted to the right for transparency, represent the results of our full calculation [31], including pions. Our results in the irrep $A_2(4)$ are predictions.

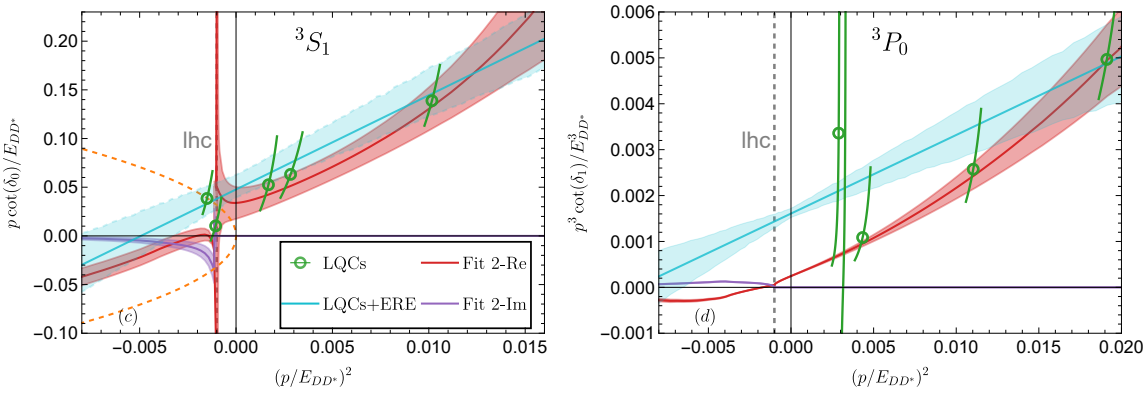

Figure 4: DD^* scattering phase shifts, in the $^3S_1$ (left panel) and $^3P_0$ (right panel) partial waves extracted from the lattice FV energy levels in Ref. [31]. Red bands represent the results of our 3-parameter fits to the lattice spectra including the OPE (see orange dots in Fig. 3), while blue bands are the 4-parameter ERE-based results of Ref. [22]; see [31] for additional details. Green dots stand for the results from the Lüscher method.

main advantage lies in the explicit account for the longest-range interactions, including the leading left-hand cut from the OPE, which is essential for maintaining the correct analytic structure of the DD^* scattering amplitude near the threshold. In this approach, finite-volume energy levels can be directly calculated as solutions to the eigenvalue problem for each lattice irrep,

$$\det\left[\mathbb{G}^{-1}(E) - \mathbb{V}(E)\right] = 0, \tag{5}$$

both below and above the left-hand cut. Importantly, since the LECs are volume-independent, once extracted from best fits to the finite-volume spectra, they can be used to predict observables in the infinite volume, as outlined in Sec. 2. Additionally, we emphasize that we use the plane wave basis instead of the conventional partial wave expansion, that facilitates the systematic inclusion of partial wave mixing effects arising from rotational symmetry breaking in a cubic box [31, 43]. We also

note that the three-body cut at this pion mass appears at a higher energy, making it irrelevant for the current study.

The results of our best fits at $O(Q^2)$ in χEFT to the lattice energy spectra of Ref. [22] are shown in Fig. 3. In addition to the S-wave interaction introduced in Eq. (1), we also included one $O(Q^2)$ contact term in the $^3P_0$ partial wave, as required in the $A_1^-(0)$ irrep. Based on this fit, we extracted the phase shifts, as shown in Fig. 4. These results demonstrate the important role of the OPE, which not only drives the energy dependence of the P-wave phase shift, but also reveals itself significantly in the S-wave near the lhc. Our analysis suggests that the T_{cc} at this pion mass is most likely a resonance, with a smaller probability of being a virtual state. For details on the pole position, the ERE parameters, and the discussion of statistical and systematic uncertainties, see [31].

5. Pion mass dependence of the T_{cc} pole position

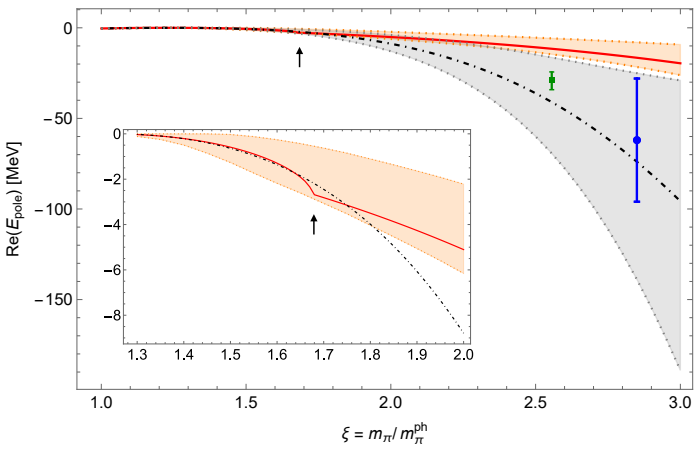

Figure 5: Comparison of the T_{cc} pole trajectory at NLO in chiral EFT with pions (red line for the best fit and orange band for 1σ statistical uncertainty) with that in a pionless theory (dot-dashed line and grey band). The arrow indicates the pion mass ($\xi \approx 1.68$) where the pole in the pionful theory transitions to a resonance. The blue point represents a virtual state extracted at $m_\pi = 391\,\text{MeV}$ [24], and the green square denotes a virtual state at $m_\pi \approx 348.5\,\text{MeV}$ extracted using the ERE parameters from Ref. [23].

With all the LECs at $O(Q^2)$ determined from our analyses of the LHCb data (C_0) and the lattice spectra at $m_\pi = 280\,\text{MeV}$ (C_2 and D_2), and with all relevant cuts incorporated in our framework, we are able to predict the behavior of the T_{cc} pole as a function of the light-quark (pion) mass. This study was conducted in Ref. [35], with an illustration provided in Fig. 5. The T_{cc} pole trajectory (red line and orange band) exhibits a remarkable evolution completely consistent with its molecular nature [41]: it transitions from a quasi-bound state at m_π^{ph} (where T_{cc} can decay to $DD\pi$ due to the three-body cut) to a bound state when the pion mass increases by approximately 3%, at $m_\pi \simeq 1.03 m_\pi^{\text{ph}}$. As the pion mass further increases, the state becomes virtual at $m_\pi \simeq 1.25 m_\pi^{\text{ph}}$, and finally transitions to a resonance at $m_\pi \simeq 1.7 m_\pi^{\text{ph}}$. The transition to a resonance highlights the significant role of the OPE, as the pole in a pure contact theory without pions remains a virtual state. Remarkably, our pionless trajectory is fully in line with the poles extracted from lattice investigations [23] at $m_\pi \simeq 350$ MeV and [24] $m_\pi \simeq 391$ MeV, both of which were carried out ignoring the OPE. These findings are represented by the grey band as well as the green and blue data points, respectively.

6. Summary

A model-independent framework based on chiral effective field theory (χEFT) is used to extract low-energy observables, such as DD^* scattering amplitudes, at both physical and larger-than-physical pion masses [13, 31, 34, 35]. The framework incorporates the longest-range one-pion exchange interaction, including all relevant cuts, which is shown to play a significant role. The light-quark mass dependence of the T_{cc} pole position is predicted up to $O(Q^2)$ in χEFT, consistent with its interpretation as a hadronic molecule. A careful analysis of various sources of uncertainty is performed, as detailed in Refs. [31, 35].

Acknoweledgments: I would like to thank Michael Abolnikov, Xiang-Kun Dong, Meng-Lin Du, Evgeny Epelbaum, Arseniy Filin, Ashot Gasparyan, Feng-Kun Guo, Christoph Hanhart, Lu Meng, Alexey Nefediev, Juan Nieves, Qian Wang for a highly enjoyable and educative collaboration, which led to the results presented in this Proceedings.

References

[1] A. Esposito, A. Pilloni, A. D. Polosa, Phys. Rept. 668 (2017) 1–97.

[2] R. F. Lebed, R. E. Mitchell, E. S. Swanson, Heavy-Quark QCD Exotica, Prog. Part. Nucl. Phys. 93 (2017) 143–194.

[3] F.-K. Guo et al., Rev. Mod. Phys. 90 (1) (2018) 015004.

[4] Y. Yamaguchi et al., J. Phys. G 47 (5) (2020) 053001.

[5] N. Brambilla et al., Phys. Rept. 873 (2020) 1–154.

[6] F.-K. Guo, X.-H. Liu, S. Sakai, Prog. Part. Nucl. Phys. 112 (2020) 103757.

[7] H.-X. Chen et al., Rept. Prog. Phys. 86 (2) (2023) 026201.

[8] L. Meng et al., Phys. Rept. 1019 (2023) 1–149.

[9] R. Aaij, et al., Nature Phys. 18 (7) (2022) 751–754.

[10] R. Aaij, et al., Nature Commun. 13 (1) (2022) 3351.

[11] M. Albaladejo, Phys. Lett. B 829 (2022) 137052.

[12] L. Meng et al., Phys. Rev. D 104 (5) (2021) 051502.

[13] M.-L. Du et al., Phys. Rev. D 105 (1) (2022) 014024.

[14] E. Braaten et al., Phys. Rev. D 106 (3) (2022) 034033.

[15] B. Wang, L. Meng, Phys. Rev. D 107 (9) (2023) 094002.

[16] L. Dai et al., Phys. Rev. D 107 (7) (2023) 076001.

[17] S. Aoki, T. Doi, Front. in Phys. 8 (2020) 307.

[18] M. Mai, M. Döring, A. Rusetsky, Eur. Phys. J. ST 230 (6) (2021) 1623–1643.

[19] P. Bicudo, Phys. Rept. 1039 (2023) 1–49.

[20] J. Bulava, et al., Hadron Spectroscopy with Lattice QCD, in: Snowmass 2021, 2022. arXiv:2203.03230.

[21] S. Prelovsek, Nuovo Cim. C 47 (4) (2024) 147.

[22] M. Padmanath, S. Prelovsek, Phys. Rev. Lett. 129 (3) (2022) 032002.

[23] S. Chen et al., Phys. Lett. B 833 (2022) 137391.

[24] T. Whyte, D. J. Wilson, C. E. Thomas, arXiv:2405.15741.

[25] S. Collins et al., Phys. Rev. D 109 (9) (2024) 094509.

[26] Y. Lyu et al., Phys. Rev. Lett. 131 (16) (2023) 161901.

[27] L. Meng et al., [arXiv:2411.06266 [hep-lat]].

[28] A. B. a. Raposo, M. T. Hansen, JHEP 08 (2024) 075.

[29] S. M. Dawid, M. H. E. Islam, R. A. Briceño, Phys. Rev. D 108 (3) (2023) 034016.

[30] J. R. Green et al., Phys. Rev. Lett. 127 (24) (2021) 242003.

[31] L. Meng et al., Phys. Rev. D 109 (7) (2024) L071506.

[32] R. Bubna et al., JHEP 05 (2024) 168.

[33] M. T. Hansen, F. Romero-López, S. R. Sharpe, JHEP 06 (2024) 051.

[34] M.-L. Du et al., Phys. Rev. Lett. 131 (13) (2023) 131903.

[35] M. Abolnikov et al., [arXiv:2407.04649 [hep-ph]].

[36] J.T. Chacko et al., arXiv:2411.13303 [hep-ph].

[37] V. Baru et al., Phys. Lett. B 726 (2013) 537–543.

[38] V. Baru et al., Phys. Rev. D 92 (11) (2015) 114016.

[39] V. Baru et al., Phys. Lett. B 763 (2016) 20–28.

[40] V. Baru et al., Phys. Rev. D 99 (9) (2019) 094013.

[41] I. Matuschek et al, Eur. Phys. J. A 57 (3) (2021) 101.

[42] V. Baru et al., Phys. Lett. B **833**, 137290 (2022)

[43] L. Meng and E. Epelbaum, JHEP **10**, 051 (2021)